# Supplemental Material:
Unifying microscopic mechanism for pressure and cold denaturations of proteins

Cristiano L. Dias

May 29, 2012

In our manuscript we discuss the unfolding of proteins at low temperature and high pressure. We show that these transitions can be modeled qualitatively using a bead and spring model embedded in explicit water. The behavior of this system can be further reduced to a system made of two non-polar molecules in explicit water. This hydrophobic dimer model constitutes one of the simplest system capable of reproducing cold and pressure denaturation. Here we show that the features of the dimer model required to account for pressure denaturation is also present in three-dimensional all-atom simulations of two methanes. In particular we show that increasing pressure stabilizes ssc.

Furthermore, using all-atom simulations, we show that the distribution of distance between side-chains ($C_\beta$ atoms) in a poly-alanine peptide whose backbone is constrain to secondary structures ($\beta$-sheets and $\alpha$-helices) is strongly populated by ssc. This result supports our claim that ssc plays an important role in the solvation of secondary structures.

## 1 PMF of a methane dimer in three dimensions

In this section we show that main changes in the PMF of two hydrophobic particles with increasing pressure – seen in our 2D model (Fig. 4b in the manuscript) – are preserved in three dimensions. Similar calculations have been reported previously by Hummer et al. [5] and Ghosh et al. [3]. The former used the distribution of cavities in pure SPC/E water to compute the PMF through the information theory and the later was simulated at constant volume using 8 methane molecules in TIP3P water. Here we perform additional simulations using TIP4P water molecules and two methanes at constant temperature and pressure. Umbrella Sampling is used to produce accurate results [1].

In Fig. 1 we show the PMF of two methanes as a function of their separation in explicit TIP4P water at pressures of 1, 1000, 2000, 3000 and 4000 atm. We use the all atom OPLSS-AA force field to describe methane molecules. Our simulation box comprises 1077 water and its size is determined using the Parrinello-Rahman barostat to account for constant pressure as implemented in GROMACS. The temperature of the

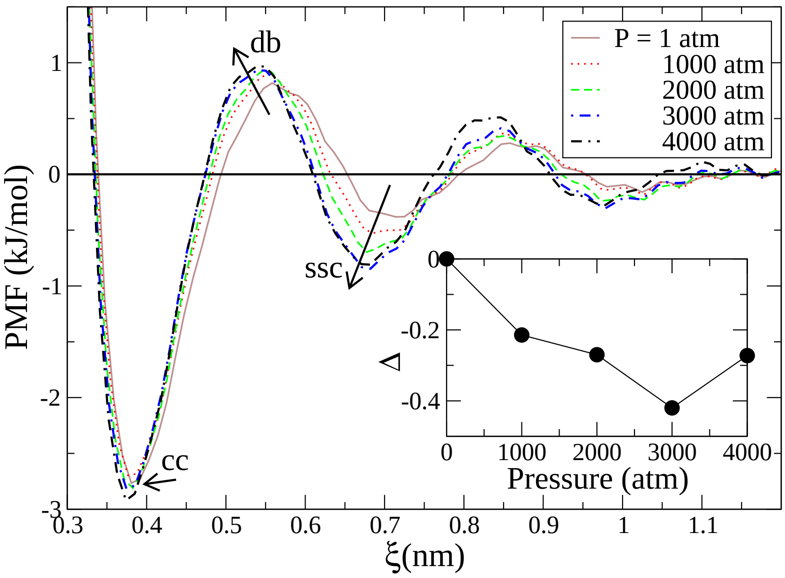

Figure 1: (Color Online) Dependence of the Potential of Mean Force (PMF) on pressure as a function of dimer distance $\xi$. Changes in the PMF at contact-configurations (cc), desolvation-configurations (db) and solvent-separated-configurations (ssc) are indicated by arrows. (INSET) Pressure dependence of the difference $\Delta$ between the PMFs at ssc and cc. This difference computed at P=1 atm is used as reference.

system is set to 298 K using the velocity-rescaling thermostat and electrostatic forces are computed using the Particle-Mesh Ewald method.

To compute the PMF we use Umbrella Sampling by applying a *bias* harmonic potential to constrain the two methanes to fix distances. We use 8000 kJ $\cdot$ mol$^{-1}\cdot$ nm$^{-2}$ for the spring constant and 20 sampling windows in which equilibrium distances of the spring are 0.3, 0.35, 0.4, 0.45,...., 1.1, 1.15, 1.2 nm. Each of these windows are sampled for 30 ns to compute the *biased* distribution of methane-methane distances. The desired unbiased distribution $p^o(r)$ required to compute the PMF is obtained by solving the WHAM (Weighted Histogram Analysis Method) equations iteratively – see, for example, reference [7] for a comprehensive discussion of the WHAM method. The PMF is obtained from:

$$\mathrm{PMF}(r) = -k_b T \log\left(\frac{p^o(r)}{r^2}\right) + \mathrm{Const.} \tag{1}$$

The region 1.15–1.20 nm is used as a baseline to superimpose the PMFs computed at different pressures. The protocol used here is very similar to the one adopted by Czaplewski et al. [1].

In Fig. 1 we show that the distances between solutes is preferred when they are in contact ($\xi \approx 0.38$ nm) and solvent-separated ($\xi \approx 0.67$ nm) [9]. At all studied pressures, the lowest PMF occurs at cc (most probable methane-methane distance) and the second lowest PMF occurs at ssc. As pressure increases, the PMF at cc remains unchanged while the PMF at ssc decreases, implying that ssc distances become more probable with increasing pressure. This result is highlighted in the inset of Fig. 1 where the difference $\Delta$ between the PMFs at ssc and cc is shown to decrease with increasing pressure.

The main feature required to explain pressure denaturation is a decrease in $\Delta$ with increasing pressure (see inset of Fig. 1). This feature is preserved in all models studied to date: our 2DMB model (Fig. 4 of our manuscript), calculations using SPC/E water models [5] and simulations using TIP3P water models [3]. This robust feature emerges from all models and can be explained by the fact that ssc configurations occupy the lowest volume (see Fig. 4c of our manuscript) and are therefore preferred at high pressure. However, details in the PMF are model dependent. This is the case for the PMF at cc which in some calculations (Fig. 4 of our manuscript and reference [5]) increases with increasing pressure while in other calculations it remains almost unchanged and even decreases slightly (Fig. 1 and reference [3]). While further calculations are needed to resolve this controversy, the latter calculations use more realistic models and more accurate methods for the PMF.

## 2 ssc in $\alpha$-helices and $\beta$-sheets

In this section we perform all-atom simulations to show that ssc plays an important role in secondary structure formation and specifically in $\beta$-sheets. We simulate polyalanine ($NH_2A_{16}COOH$) embedded in a box containing TIP4P water molecules using the OPLSS-AA force-field. Temperature is kept constant at 298 K using the velocity-rescale thermostat and pressure is tunned to 1 atm with the Parrinello-Rahman barostat. We perform two sets of simulations. In the first set $C_\alpha$ atoms are restrained to a $\beta$-sheet and in the second set they are restrain to an $\alpha$-helix. Water molecules and sidechains are free to move during the simulation. Initial peptide conformations are taken from our previous work [2] and relaxed with the OPLSS-AA force-field in vacuum using a steepest descent method. Water is added to the system such as to form a solvation shell of 1.2 nm thickness around the peptide. The first 250 ps of the simulation are ignored and the next 60 ns used for analyses. Atomic configurations are saved every 2 ps. Typical peptide conformations are shown in Fig. 2.

As the hydrophobic interaction between molecules depends on their distance (see Fig. 1), we study here the distance distributions between $C_\beta$ atoms in $\alpha$-helix (full line in Fig. 3) and $\beta$-sheet (dashed line). In Fig. 3(b) we show the different length-scales associated with the hydrophobic interaction of small non-polar molecules by plotting the PMF of methane association at 298 K and 1 atm. Shaded regions correspond to contact configurations (cc), desolvation barrier (db) and solvent separated configurations (ssc).

The main peak in the distance distribution of $\beta$-sheets is associated with interactions between residues $i, i+2$ (see Fig. 2). This peak occurs at ssc distances and therefore contributes favorably to the energy of $\beta$-sheets. Furthermore, since the PMF at ssc decreases with increasing pressure (see Fig. 1), the contribution of this first peak stabilizes

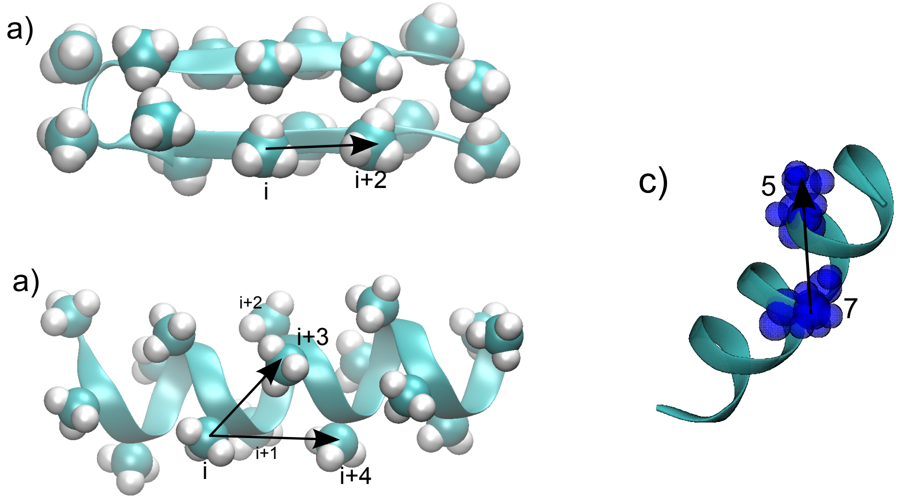

Figure 2: (Color Online) Characteristic configurations of $\beta$-sheet (a) and $\alpha$-helix (b-c). Relevant distances accounting for peaks in Fig. 3(a) are shown by arrows. Panel (c) illustrates relative positions of residues $i$ and $i+2$ within the $\alpha$-helix (for $i = 5$).

$\beta$-sheets with increasing pressure.

The first two peaks of the $\alpha$-helix are associated with interactions between residues $i, i+3$ and between $i, i+4$ (see Fig. 2). These peaks occur at db distances and, therefore, contribute unfavorably to the energy of an $\alpha$-helix. Furthermore, since the PMF at db increases with increasing pressure, the energetic penalty related to these interactions also increases with increasing pressure. An opposing effect to the db penalty could come from the third peak in $\alpha$-helices. This third peak occurs at distances associated to ssc and therefore could contribute favorably to the energy of an $\alpha$-helix. However, this third peak corresponds to interactions between residues $i, i+2$ which are diametrically opposed along the axis of the $\alpha$-helix (see Fig. 2c). In this configuration, residues $i$ and $i+2$ are not separated by water molecules as in standard ssc configurations. Hence, the PMF of methane association at ssc should not be used to describe the third peak, and it is not clear whether this third peak contribute favorably or unfavorably to $\alpha$-helix.

Based on similar analyses, Dias et Chan [2] have suggested a possible scenario to explain why some amyloid peptides form $\beta$ or coil conformations in water but they adopt $\alpha$-helical conformations in membrane mimicking environments [4]. In their explanation, desolvation effects would penalize $\alpha$-helix vis-à-vis $\beta$-sheet in water while these effects would be absent in membrane-like environment where hydrogen bonds could favor $\alpha$-helix. Our present results (Fig. 3) support their findings and suggest further that increasing pressure causes hydrophobic interactions to stabilize $\beta$-sheets. As a matter of fact, pressure has been shown to favor the formation of fibrilar structures composed mainly of $\beta$-sheets in amyloid peptides [10, 6]. Our results also suggest that some secondary structures, e.g., $\beta$-sheet, could survive pressure denaturation and remain stable

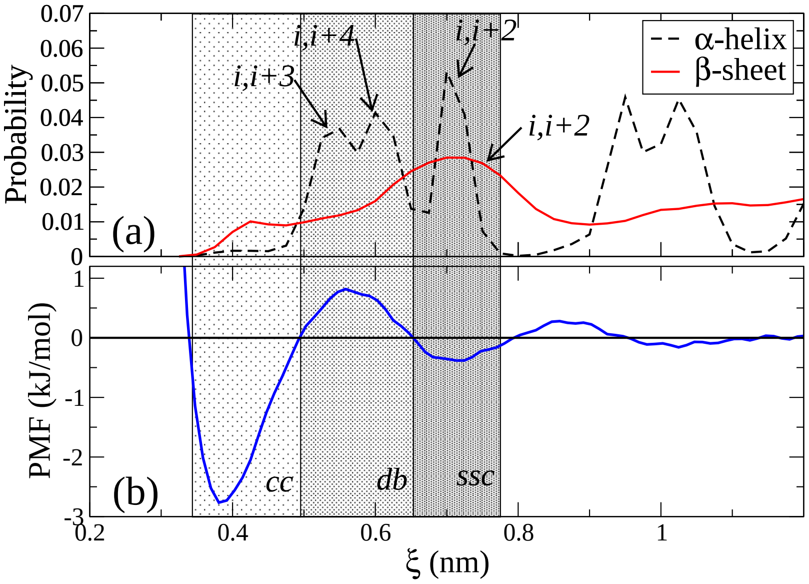

Figure 3: (Color Online) (a) Distance probability of side chains ($C_\beta$ atoms) in a polyalanine peptide restrain to $\alpha$-helix (dashed line) and $\beta$-sheet (full line) conformations. First, second and third peaks in $\alpha$-helices correspond to interactions between residues *i,i+3* , *i,i+4*, and *i,i+2*, respectively. First peak in $\beta$-sheets corresponds to interactions between residues *i,i+2*. (b) Potential of mean force between two methanes at T = 298 K and P = 1 atm. Interaction distances corresponding to contact configurations (cc), desolvation barrier (db), and solvent-separated-configurations (ssc) are shaded.

even after the dry core of the protein has been hydrated [8, 11].

## References

[1] Cezary Czaplewski, Sylwia Rodziewicz-Motowidlo, Magdalena Dabal, Adam Liwo, Daniel R. Ripoll, and Harold A. Scheraga. Molecular simulation study of cooperativity in hydrophobic association: clusters of four hydrophobic particles. *Biophys. Chem.*, 105:339, 2003.

[2] Cristiano L. Dias, Mikko Karttunen, and Hue Sun Chan. Hydrophobic interactions in the formation of secondary structures in small peptides. *Physical Review E*, 84(4):041931, 2011.

[3] Tuhin Ghosh, Angel E. García, and Shekhar Garde. Molecular dynamics simulations of pressure effects on hydrophobic interactions. *J. Am. Chem. Soc.*, 123(44):10997–11003, 2001.

[4] Jonathan Heller, Andrew C. Kolbert, Matthias Ernst Russell Larsen and, Tatiana Bekker, Michael Baldwin, Stanley B. Prusiner, Alexander Pines, and David E. Wemmer. Solid-state nmr studies of the prion protein h1 fragment. *Protein Science*, 5:1655, 1996.

[5] Gerhard Hummer, Shekhar Garde, Angel E. García, Michael E. Paulaitis, and Lawrence R. Pratt. The pressure dependence of hydrophobic interactions is consistent with the observed pressure denaturation of proteins. *Proceedings of the National Academy of Sciences*, 95(4):1552 –1555, February 1998.

[6] Ralf Jansen, Stefan Grudzielanek, Wojciech Dzwolak, and Roland Winter. High pressure promotes circularly shaped insulin amyloid. *Journal of Molecular Biology*, 338:203, 2004.

[7] Shankar Kumar, John M. Rosenberg, Djamal Bouzida, Robert H. Swendsen, and Peter A. Kollman. The weighted histogram analysis method for free-energy calculations on biomolecules. i. the method. *Journal of Computational Chemistry*, 13:1011, 1992.

[8] Filip Meersman, Lászó Smeller, and Karel Heremans. Comparative fourier transform infrared spectroscopy study of cold-, pressure-, and heat-induced unfolding and aggregation of myoglobin. *Biophysical Journal*, 82(5):2635, 2002.

[9] L. R. Pratt and D. Chandler. *J. Chem. Phys.*, 67:3683, 1977.

[10] Joan Torrent, Maria Teresa Alvarez-Martinez, Marie-Cécile Harricane, Frédéric Heitz, Jean-Pierre Liautard, Claude Balny, and Reinhard Lange. High pressure induces scrapie-like prion protein misfolding and amyloid fibril formation. *Biochemistry*, 43(22):7162–7170, 2004.

[11] Roland Winter, Dahabada Lopes, Stefan Grudzielanek, and Karsten Vogtt. Towards an understanding of the temperature/ pressure configurational and Free-Energy landscape of biomolecules. *Journal of Non-Equilibrium Thermodynamics*, 32:41–97, 2007.